International Journal of Coal Geology 164 (2016) 35–47

Contents lists available at ScienceDirect

International Journal of Coal Geology

journal homepage: www.elsevier.com/locate/ijcoalgeo

Characterisation of hydraulic and hydrogeochemical processes in a reducing and alkalinity-producing system (RAPS) treating mine drainage, South Wales, UK

Kate Taylor [a], David Banks [b,*], Ian Watson [c]

[a] Easternwell, Level 4, 52 Merivale Street, South Brisbane, Queensland 4101, Australia
[b] School of Engineering, James Watt Building (South), University of Glasgow, Glasgow G12 8QQ, United Kingdom
[c] The Coal Authority, 200 Lichfield Lane, Mansfield, Nottinghamshire NG18 4RG, United Kingdom

ARTICLE INFO

Article history:
Received 7 July 2015
Received in revised form 18 April 2016
Accepted 13 May 2016
Available online 16 May 2016

Keywords:
Tracer test
Alkalinity
Mine water
Artificial wetland
Matrix diffusion
Ion exchange

ABSTRACT

A series of tracer tests has been carried out in the compost and limestone Tan-y-Garn Reducing and Alkalinity-Producing System (RAPS), designed to treat iron-rich net acidic mine water (mean pH 6.18, Fe = 47 mg L^{-1}, alkalinity 1.70 meq L^{-1} and mineral acidity 1.82 meq L^{-1}) in South Wales, UK. Conservative tracer breakthrough time in the RAPS basal effluent is approximately inversely related to throughflow rate. Repeat tracer tests indicate a long term decrease in hydraulic conductivity, but not in total porosity.

A specific sodium chloride tracer test from June 2008 is reported, when 15 kg salt was added to a raw mine water inflow rate of 0.87 L s^{-1}. Electrical conductivity and major ion chemistry were monitored for a 170 h period. Sodium exhibited a retardation of 1.15 to 1.2 in the RAPS medium relative to chloride, due to cation exchange. Simple 1-D advection-diffusion analytical modelling succeeded in simulating the early portion of tracer breakthrough in the RAPS effluent. More complex analytical modelling, accounting for (i) mixing and dilution effects in the supernatant water input signature and (ii) matrix diffusion effects, was found to be required to adequately simulate the later-stage tail of the breakthrough curve in the RAPS effluent.

© 2016 Elsevier B.V. All rights reserved.

1. Introduction

1.1. What is a reducing and alkalinity-producing system (RAPS)?

It is common and cost-effective to treat iron-rich mine waters (Banks and Banks, 2001; PIRAMID Consortium, 2003; Sapsford and Watson, 2011) by passive, aerobic methods, such as aerobic sedimentation basins or wetlands. These function by the oxidation of ferrous to ferric iron, followed by the hydrolysis and precipitation of ferric iron from the water. This net process can be described by Eq. (1):

$$4Fe^{2+} + O_2 + 4H^+ + 10H_2O = 4Fe^{3+} + 12H_2O = 4Fe(OH)_3 + 12H^+ \quad (1)$$

The overall oxidation and hydrolysis reaction is thus acid-producing (2 mol of protons released for every mole of ferrous iron oxidised and precipitated). However, the hydrolysis and precipitation reaction is strongly pH-dependent: if the pH becomes too low, the hydroxide precipitate will not form. Thus, it is important that sufficient alkalinity is available in the water to absorb the protons produced and to buffer the pH at a reasonably high level (Hedin et al., 1994a; Younger et al., 2002). Alkalinity can be added actively, by dosing the influent mine water with hydroxide or carbonate. However, it can also be released passively by allowing the mine water to flow through limestone drains before entering the aerobic treatment lagoons or wetlands (PIRAMID Consortium, 2003). The limestone slowly dissolves, releasing bicarbonate alkalinity to the water. If the water contains oxygen, however, ferric hydroxide may precipitate out in the limestone drains, "armouring" the limestone clasts and inhibiting further dissolution (Hedin et al., 1994b; Cravotta and Trahan, 1999; Watzlaf et al., 2000a; Bernier et al., 2001). Thus, it is important to strip oxygen from the water before it enters the limestone drain, ensuring that iron remains in its ferrous form (Eq. (2)). This is most effectively done by a layer with a high organic content and thus a high oxygen demand - for example, a compost layer (represented by CH_2O in Eq. (2)).

$$4Fe^{2+} + O_2 + CH_2O + CaCO_3 = Ca^{++} + 2HCO_3^- + 4Fe^{2+} \quad (2)$$

Such a Reducing and Alkalinity-Producing System, or RAPS (Kepler and McCleary, 1994; Watzlaf et al., 2000b; Younger et al., 2002; Amos and Younger, 2003; PIRAMID Consortium, 2003; Fabian et al., 2005) can thus be used as a pre-treatment step in the passive aerobic treatment of acidic/ferruginous mine drainage water. It comprises either:

* Corresponding author.
E-mail address: david@holymoor.co.uk (D. Banks).

http://dx.doi.org/10.1016/j.coal.2016.05.007
0166-5162/© 2016 Elsevier B.V. All rights reserved.

Table 1
Physico-chemical properties of mine water at Tan-y-Garn (arithmetic means cited). Changes through the RAPS are shown as percentages of the raw (input) average concentration, with the exception of figures marked *, which are in the cited units. Parameters showing a significant decrease through the RAPS are shaded. Modified after Watson et al. (2009).

Parameter	Unit	Raw mine water			RAPS outflow			Change
		Mean	St.dev.	N	Mean	St.dev.	N	
Flow	L/s	2.05	1.38	81	1.89	1.22	81	
Temperature	°C	11.05	1.10	59	11.84	2.87	59	+0.79*
Total organic carbon	mg L^{-1} as C	0.94	0.38	51	2.89	2.46	55	+207%
pH		6.18	0.22	60	7.01	0.22	57	+0.83*
Dissolved Oxygen	mg/L^{-1}	1.29	0.60	53	2.10	1.18	53	+63%
Electrical Conductivity	µS cm^{-1}	673.1	32.7	59	841.4	62.9	57	+25%
Eh	mV	−13.3	28.6	55	−92.3	43.3	54	−79*
Field alkalinity	meq/L^{-1}	1.70	0.30	60	4.58	0.51	59	+169%
Sulphate	mg/L^{-1} as SO_4	254.2	13.1	60	227.8	33.0	61	−10%
Chloride	mg/L^{-1}	12.5	1.4	61	12.2	1.9	57	−2%
Calcium	mg/L^{-1}	42.9	2.2	61	121.8	14.2	59	+184%
Magnesium	mg/L^{-1}	29.1	1.6	60	29.2	2.4	59	0%
Sodium	mg/L^{-1}	10.3	1.1	60	11.1	2.7	59	+9%
Potassium	mg/L^{-1}	6.4	1.8	61	6.6	1.2	59	+3%
Manganese	mg/L^{-1}	3.64	3.36	61	2.90	0.90	57	−20%
Aluminium	mg/L^{-1}	0.13	0.09	59	0.03	0.06	43	−77%
Ferrous Iron	mg/L^{-1}	46.23	2.60	60	7.07	4.14	57	−85%
Total Iron	mg/L^{-1}	46.60	3.91	60	7.14	3.85	58	−85%
Iron Loading	kg/day^{-1}	8.27	0.47	42	1.16	1.05	42	−86%

(i) A layer of compost (or other organic waste) over a porous limestone (or other carbonate lithology) drain, or
(ii) A mixed porous medium comprising compost and limestone clasts, or
(iii) A composite structure containing layers of limestone fragments and compost

If the RAPS becomes excessively reducing, bacterially mediated sulphate reduction can also occur, which can lead to generation of hydrogen sulphide gas and/or to precipitation of metals (Me in Eq.. (3)) as solid sulphide phases within the RAPS:

$$SO_4^{=} + 2CH_2O + 2CaCO_3 + Me^{++} = MeS + 4HCO_3^{-} + 2Ca^{++} \quad (3)$$

On exiting a RAPS, the mine water will typically:

(i) Pass through a re-aeration system, such as an aeration cascade, before entering
(ii) A system of aerobic treatment lagoons and/or wetlands, where the iron content of the water is removed by the reactions in Eq.. (1).

RAPS have typically been applied to iron-rich, net-acidic coal mine waters.

1.2. The Tan-y-Garn site

Tan-y-Garn was a small drift colliery at Garnswllt, Ammanford, Carmarthenshire, South Wales, UK (51.7696°N 3.9849°W; OSGB36 Grid reference SN 6313 0973). The mine complex underlies a total area of less than 0.3 km^2 and worked the "Ynysarwed" coal seam from 1876 to 1990. The "Ynysarwed seam" is often taken to be synonymous with what is currently referred to as the Rhondda No. 2 seam (Strahan et al., 1907), although the naming of seams has historically been somewhat arbitrary and problematic to tally with current accepted nomenclature. In the specific case of Tan-y-Garn, it seems more likely that the seam worked was the stratigraphically slightly higher Rhondda No. 1 (or Duke) seam (see the published geological map by BGS, 1977 and the report by SRK, 1994). Both the Rhondda No. 1 and No. 2 seams lie in the Rhondda Beds member of the Lower Pennant Measures of the Westphalian Upper Coal Measures. The seams are associated with a relatively thick sandstone unit with subordinate silts and shales. The worked seam was recorded as 2 ft. 11 in. (89 cm) thick at "Old Garn Swllt" colliery by Strahan et al. (1907). The local dip of strata is between 10° and 17°S to SW according to BGS (1977).

Following abandonment in around 1990, the Tan-y-Garn workings flooded, and overflowed via a mine entrance as a polluting ferruginous discharge to the south side of the local stream, the Afon Cathan. The workings of Tan-y-Garn are estimated to underlie an area of c. 0.12 km^2 and are located south of the mine water discharge point on the south side of the River Cathan. They thus lie below the discharge level, reaching down to elevations of −30 m below sea level and are presumed to be flooded. The mine was connected to the adjacent

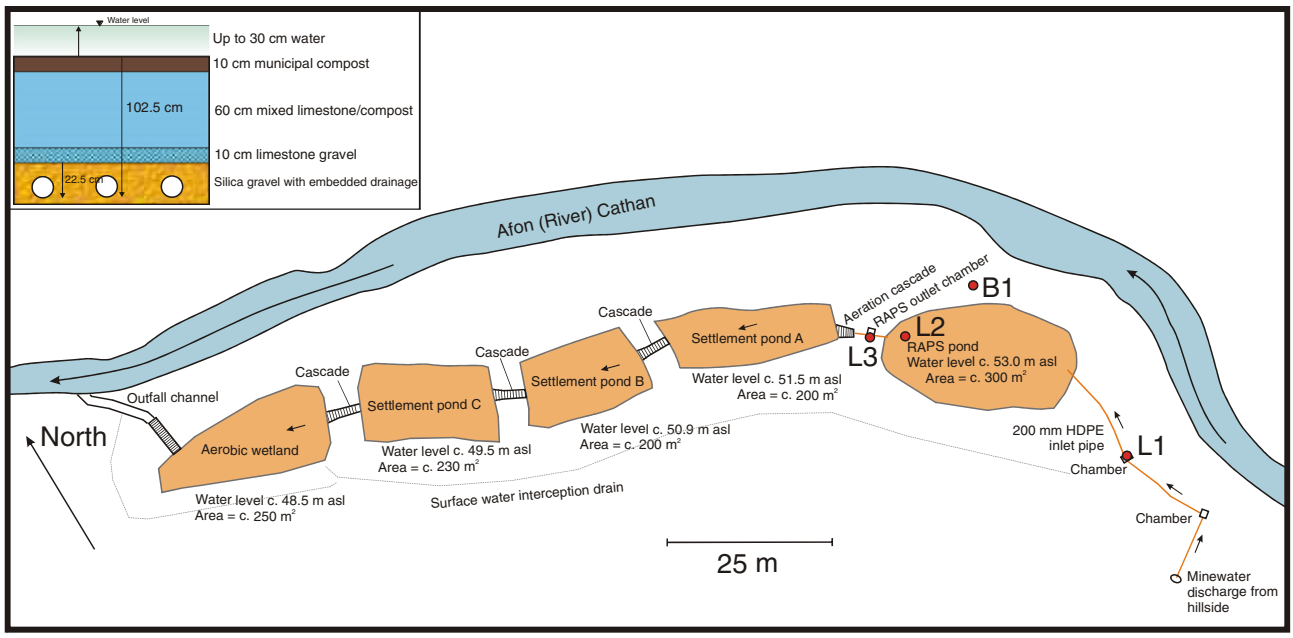

Fig. 1. Outline map of Tan-y-Garn mine water treatment system showing logger locations L1-L3 and B1. Tracer injection at L1. Based on maps in Atkins (2006). Inset shows cross-section of RAPS structure. HDPE = high density polyethylene.

Garnswllt colliery (SRK, 1994) to the west of the discharge point The Garnswllt workings, of very limited areal extent (0.017 km^2), being largely above the discharge level, are assumed to be unflooded.

The discharging mine water at the site has a typical flow rate of 2 L s^{-1} (equating to around 451 mm of annual recharge, distributed over a worked area of c. 140,000 m^2, for a location with an estimated annual average precipitation of 1265 mm), although this can vary significantly with rainfall from 0.5 to 5 L s^{-1}.

Shortly after the mine flooded and overflowed, SRK (1994) recorded iron concentrations of around 72 mg L^{-1}, pH of 5.7 and sulphate of 480 mg L^{-1}. Since then the quality has improved somewhat (Table 1), presumably as accumulated products of pyrite oxidation have been flushed out of the mine.

The Welsh coals generally have a "moderately low" sulphur content of 1 to 1.5%, according to Spears et al. (1999), citing data by Wandless (1959). The fact that the Pennant series coals are of more continental facies, as opposed to the deeper Middle Coal Measures seams, which are more commonly associated with marine bands, also suggests that their sulphur content might be expected to be modest (Lee, 1995). Greenwell and Elsden (1907) cite a sulphur content of 0.94% for the Pennant series Little Vein coal at Ammanford colliery and 0.74% sulphur for the Rhondda No. 3 coal in Glamorgan. Davies (1921) cites around 1.3% sulphur for the Rhondda No. 2 seam, also in Glamorgan.

The chemistry of the raw untreated mine water shows relatively little variation, despite rainfall-related flow variations, and is summarised in Table 1 (after Watson et al., 2009). The mine water has a pH of around 6.2 and is chemically reducing. It contains, on average 46.6 mg L^{-1} iron, of which the overwhelming majority (46.2 mg L^{-1} = 1.65 meq L^{-1}) is ferrous. The total alkalinity is on average 1.70 meq L^{-1}. On the basis of the mean values in Table 1, the total mineral acidity (non-CO_2) is calculated (Hedin et al., 1994a; PIRAMID Consortium, 2003; McAllan et al., 2009) as 1.82 meq L^{-1}. This suggested a mildly net acidic mine water that would benefit from alkalinity addition, e.g. via a RAPS, prior to treatment by aerobic oxidation and precipitation of iron (Coal Authority, 2014). Such a RAPS was thus constructed at Tan-y-Garn (Fig. 1): it commenced operation in January 2006 (Atkins, 2006; Geroni, 2011; Geroni et al., 2011) and comprises:

- Up to 30 cm of standing water. The mine water drains out of the mine tunnel into the RAPS, and ponds as supernatant water on top of the RAPS upper layer.
- 10 cm upper layer of municipal (peat-free) compost.
- 60 cm mixed layer of 50:50 vol.% municipal compost and Carboniferous limestone gravel.
- lower layer of 10 cm of Carboniferous limestone gravel.
- an underdrain, comprising silica gravel and embedded drainage pipes, of design thickness of 22.5 cm to the base of the embedded pipes. The drainage pipes feed the water into an outflow pipe.

The total RAPS thickness is thus around 1 m. The RAPS has a top surface area of around 280 m^2 as an oval shape approx 30 m by 10 m (although the liquid surface area is dependent on flow rate: if the inflow is low, the downflow through the RAPS can exceed the inflow, resulting in a drop in supernatant water level and in small areas of shoreline becoming exposed). The calcitic limestone gravel was derived from two local quarries (Ammanford and Penderyn) in the Carboniferous limestone. The gravel clast size ranged from 5 to 40 mm, with a median of just less than 20 mm. Around 180 tonnes limestone gravel were used in the RAPS (Atkins, 2007), representing 3.6×10^9 meq neutralising capacity. Based on the general characteristics of Welsh Carboniferous limestone, it is not unreasonable to assume a relatively high degree of limestone purity (Harrison, 1993).

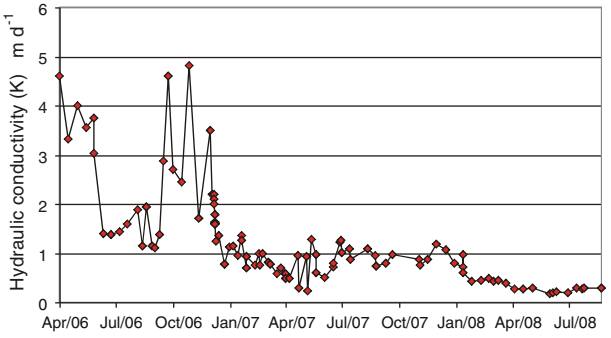

Fig. 2. Estimated change in vertical hydraulic conductivity with time for RAPS (after Watson et al., 2009).

The outflow from the RAPS is via a flexible pipe, the level of whose mouth can be adjusted. This alters the head difference across the RAPS, which can, in turn, affect the throughflow rate and the level of standing water on top of the RAPS, up to a maximum freeboard of c. 30 cm. The supernatant water level in the RAPS thus depends on the head gradient (the controlled level of the outflow pipe), the hydraulic conductivity of the RAPS media and the flow entering the system.

On leaving the RAPS, the water flows through a series of aeration cascades and three aerobic sedimentation basins, before discharging, via an aerobic wetland, to the Afon (River) Cathan (Fig. 1).

After the RAPS commenced operation, it became evident that some iron oxidation and ochre precipitation was occurring in the supernatant water of the RAPS. However, by comparing the raw mine water with the RAPS effluent, it is clear that the RAPS is fulfilling its primary function of raising the pH and alkalinity of the water, converting it to a net alkaline condition. The effluent water is almost saturated with respect to calcite and, of course, it contains elevated concentrations of calcium. Further, it contains depleted concentrations of sulphate, suggesting sulphate reduction (-26.4 mg L^{-1} or -0.55 meq L^{-1}, on average) is being facilitated by the compost in the RAPS media. The effluent water also contains decreased concentrations of iron (-39.5 mg L^{-1} or -1.4 meq L^{-1}), manganese and aluminium, suggesting hydroxide precipitation on top of (and possibly within) the RAPS, in addition to losses due to iron sulphide precipitation. See Atkins (2007), Watson et al. (2009) and Geroni (2011) for further details.

1.3. Decline in hydraulic conductivity

Assuming an average flow rate of 2 L s^{-1} (Table 1), and dividing this by the RAPS area, this implies an average Darcy velocity down through the RAPS of:

$$0.002\ m^3 s^{-1}/280\ m^2 = 7.1 \times 10^{-6}\ m\ s^{-1} = 0.62\ m\ d^{-1} \quad (4)$$

Dividing this figure by the vertical hydraulic gradient across the RAPS (i.e. the head difference between the supernatant water and the outflow pipe) yields an estimate of bulk composite vertical hydraulic conductivity. As the flow rate and head difference are regularly monitored, this allows systematic changes in hydraulic conductivity to be identified. Watson et al. (2009) report the apparent progressive deterioration of the hydraulic conductivity of the Tan-y-Garn RAPS system over the course of several years. Fig. 2 illustrates the decline in apparent hydraulic conductivity, as calculated by throughflow per unit area (Darcy velocity) divided by hydraulic gradient. By June 2008, the bulk vertical hydraulic conductivity had declined to some 0.25 m d^{-1}. As hydraulic

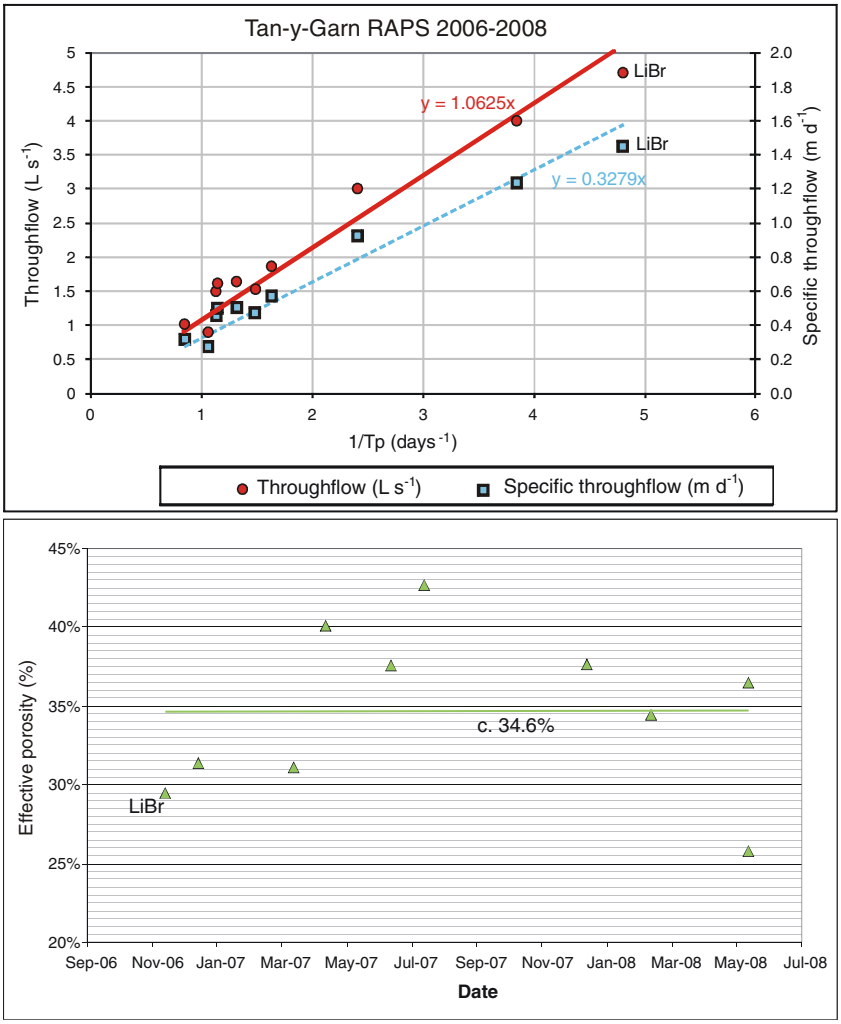

Fig. 3. Results of 10 hydraulic tracer tests performed 2006–2008; 9 tests used NaCl tracer, 1 test used LiBr (marked). The tests with the highest flow rates were generally the earliest tests. T_p = time to peak tracer concentration in effluent. Specific throughflow is calculated as throughflow divided by RAPS area of 280 m^2. In the lower diagram, there is no discernable trend: thus, the marked "trendline" should be understood as an average. Based on data presented in Watson et al. (2009).

conductivity decreases, several things happen in order to maintain RAPS throughflow:

- It becomes necessary to lower the level of the outflow pipe to increase the hydraulic gradient down through the RAPS.
- The freeboard of supernatant water above the RAPS increases (thus also increasing hydraulic gradient).
- Eventually the maximum freeboard of 30 cm is exceeded and untreated mine water begins to overflow, bypassing the RAPS, and discharging directly to the aerobic treatment lagoons (this also occurs if mine water flow rates increase beyond the RAPS capacity for meteorological reasons - i.e. high rainfall).

It is recognised that RAPS hydraulic performance (bulk vertical hydraulic conductivity) can decrease with time, due to the following potential factors:

- Post-construction compaction
- Accumulation of iron oxyhydroxide (ochre) in the supernatant layer
- Mineral precipitation and biofouling within the RAPS itself.

1.4. Previous tracer tests

Tracer tests have previously been successfully used to elucidate hydraulic conditions and modal and mean residence times in mine systems and RAPS (Aldous and Smart, 1988; Diaz-Goebes and Younger 2004; Wolkersdorfer, 2002, 2008; Wolkersdorfer et al. 2005, 2016; Watson et al. 2009). During the years 2006–2008, around ten tracer tests were carried out at Tan-y-Garn (Atkins, 2007; Watson et al., 2009) using lithium bromide, sodium chloride or fluorescein as quasi-conservative tracers. The tests showed the expected inverse linear relationship between flow rate (Q) through the RAPS and time (T_p) to peak tracer concentration in effluent (Fig. 3a). Given that

$$H/T_p = v_D/n_e, \text{ then } v_D/(1/T_p) = Hn_e \quad (5)$$

where H = the thickness of the RAPS = 1.025 m
v_D = specific discharge or Darcy velocity (m d^{-1})
n_e = effective porosity of the RAPS.

The above assumes that the RAPS medium is relatively homogenous and that T_p represents a mean conservative tracer travel time. We should note that T_p for a conservative tracer actually corresponds to a *modal* or *dominant residence* time of the system, which may not be the same as a mean residence time (Kusin et al., 2012), especially if there are significant matrix diffusion effects or a multi-modal porosity distribution.

Thus, the gradient of the graph (Fig. 3a) = 0.3279 m = 1.025 m × n_e, suggesting an effective RAPS porosity n_e of around 32%. Alternatively, we can calculate effective porosity (n_e) from each individual test (Fig. 3b). From these calculations, we obtain a first estimate of the effective bulk porosity of the RAPS at 32–35%, although this may be an overestimate, due to the finite volume of the partially ochre-filled supernatant water layer.

Fig. 3b exhibits a large variance in derived values, but fails to demonstrate any systematic trend or decline in calculated effective porosity. The fact the we observe a decline in hydraulic conductivity (Fig. 2)

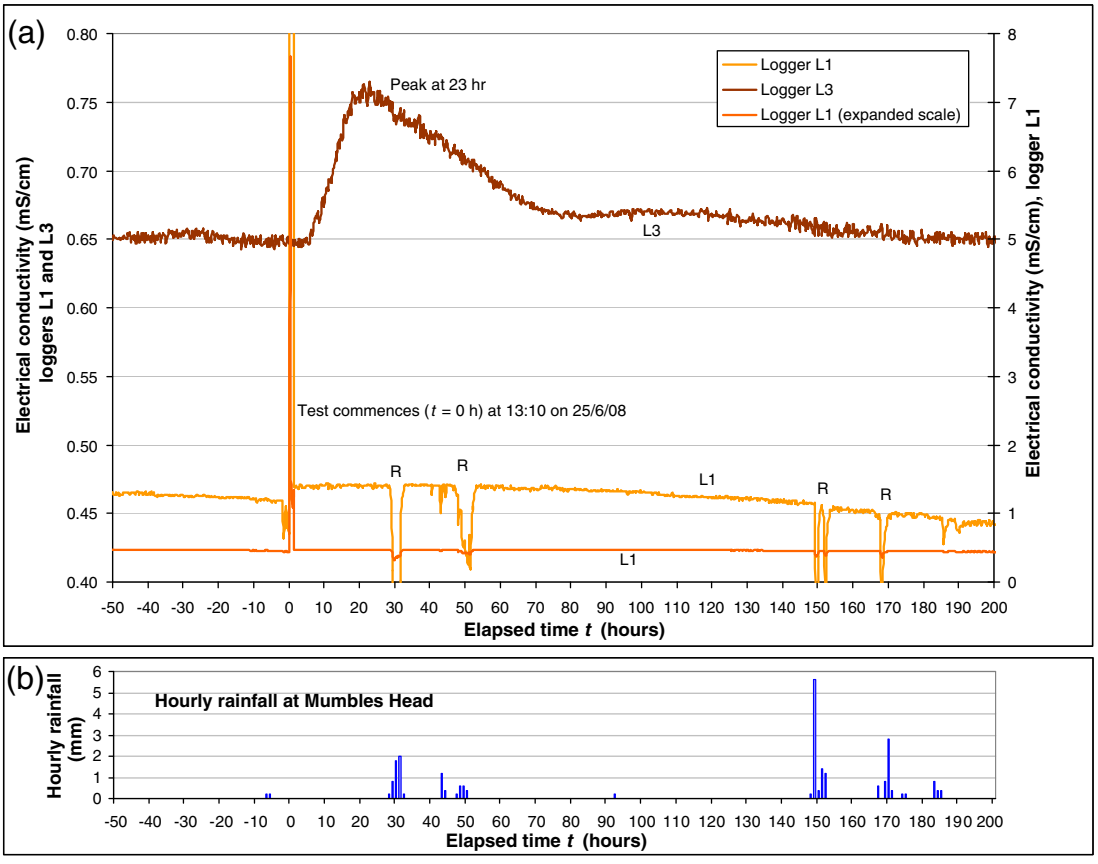

Fig. 4. (a) Electrical conductivity measurements during tracer test of June 2008 (conductivity uncorrected for temperature). Note that the peak measured conductivity in the mine water inflow chamber (L1) was around 7670 μS cm^{-1}. Tracer injection at t = 0. R denotes probable rainfall events diluting the mine water. (b) Hourly rainfall measurements for Mumbles Head meteorological station (OSGB36 Grid reference SS 627870, approximately 23 km due south of Tan-y-Garn).

without a clear decline in effective porosity (Fig. 3b) should not be too surprising, as hydraulic conductivity is controlled by the aperture of the throats (Doyen, 1988; Rezaee et al., 2006), connecting pore spaces, which can become clogged very easily, rather than by the aperture of the pores themselves (Heiderscheidt et al., 2008). The spread of values in Fig. 3b also provides some impression of the accuracy of the hydraulic data obtained from analysis of these tracer tests, approximately 30% around the mean value.

2. Methods and materials

2.1. Objective

The initial objective of the June 2008 tracer test described in this section was to carry out a combined hydraulic and thermal tracer test, by the injection of a conservative chemical (sodium chloride) and thermal signal (cool water) into the RAPS system (Taylor, 2008). The thermal behaviour of the RAPS represents a separate scientific thread and is reported in a companion paper to this (Taylor et al., *in prep.*). This paper focuses on an integrated presentation of the hydraulic and chemical behaviour of the RAPS.

2.2. Combined tracer test: June 2008

At 13:10 on 25th June 2008, a combined sodium chloride and thermal tracer (cool water) test was initiated.

Prior to the test, the influent mine water had an electrical conductivity of 460 μS cm^{-1}, while the effluent water from the RAPS was more mineralised and had an electrical conductivity of 650 μS cm^{-1}. At the time of the test, the flow rate through the RAPS was lower than the typical flow rate (cited above as around 2 L s^{-1}), reflecting the low recharge to the mine system during summer. During the 72 h period following the commencement of the tracer test, the flow varied between extremes of 0.62 to 1.13 L s^{-1}, with an arithmetic mean of 0.87 L s^{-1}, a standard deviation of 0.09 L s^{-1}, but with no systematic increasing or decreasing trend.

For the test, an empty 200 L drum was placed adjacent to the access chamber L1 (Fig. 1) down-gradient from the mine entrance from which the water emerges. 15 kg of sodium chloride (common salt, corresponding to 256 mol: 5.9 kg sodium and 9.1 kg chloride) was initially placed in the drum. From upstream of a temporary impoundment in the chamber, around 0.65 L s^{-1} of the mine water flow were pumped into the drum, which was stirred manually, dissolving the NaCl rapidly. When the drum was full, after some 300 s, the saline water from the drum was allowed to overflow via a hose back to the access chamber, downstream of the impoundment, re-joining the total mine water flux (to result in the narrow spike in electrical conductivity at L1 - Fig. 4).

2.3. Monitoring

The test was monitored by four electronic loggers (Schlumberger Water Services Diver® type) installed at the site (Fig. 1) at the following locations:

- B1 in the open air adjacent to the RAPS, measuring ambient air temperature and barometric pressure (Baro-Diver®). The readings from diver B1 were used to compensate divers L1 to L3 for atmospheric pressure.
- L1 in the "inflow chamber" receiving mine water from the mine tunnel entrance, recording water level and influent water temperature and electrical conductivity (CTD-Diver®, with a manufacturer-cited accuracy in conductivity of ±1% and a resolution of ±0.1%).
- L2 in the RAPS supernatant water, measuring water level and water temperature (Mini-Diver®), located near downstream end for reasons of access.
- L3 in the RAPS outflow chamber, measuring water level, water temperature and electrical conductivity (CTD-Diver®). A 28°4′ angle v-notch weir (Atkins, 2006) was installed in the chamber, allowing flows to be calculated from water levels in at L3, using a conversion algorithm provided by the Coal Authority. Manual readings were taken at the weir board at regular intervals to confirm logged data.

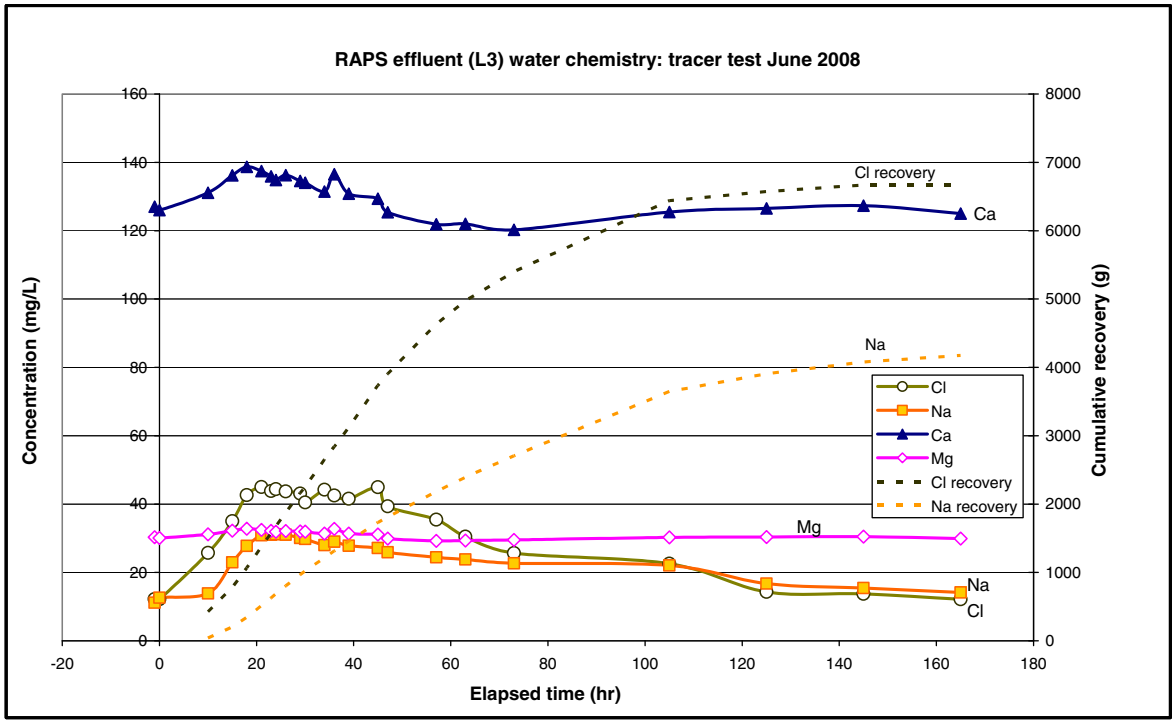

Fig. 5. Concentrations (mg L^{-1}) of Cl^-, Na^+, Ca^{++} and Mg^{++} in RAPS effluent outfall water during tracer test of June 2008. Also shown is estimated cumulative recovery of Cl^- and Na^+ (cumulative recovery corrected for background concentrations).

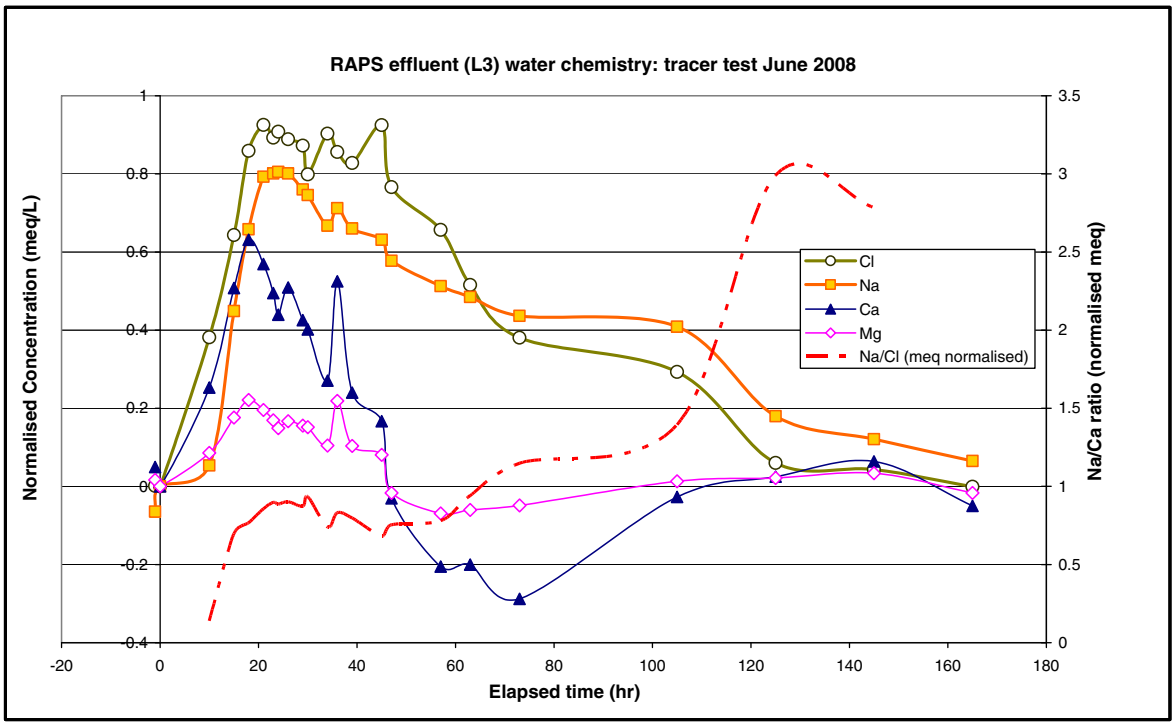

Fig. 6. Excess concentrations (normalised relative to background) of Cl^-, Na^+, Ca^{++} and Mg^{++} in RAPS effluent outfall water during tracer test of June 2008, in meq L^{-1}. Also shown is Na/Ca meq ratio (also corrected for background).

No density compensation was made to loggers L1 to L3 as the electrical conductivity at the NaCl tracer peak in the RAPS effluent only reached 750 μS cm^{-1} and the total variation over the course of the test was only 100 μS cm^{-1} (Fig. 4).

2.4. Automated sampling and analysis

An automated sampler was set up at the RAPS outflow (L3), programmed to take 500 mL water samples by activating a peristaltic pump at a frequency of 1 per hour. Samples were downloaded from the autosampler twice daily and filtered using a syringe-driven 0.2 μm cellulose acetate filter into 50 mL sample vials. Water samples were returned and submitted for analysis:

- Of total alkalinity immediately using a portable titration kit.
- For the anions Cl^-, NO_3^- and SO_4^{2-} at the Oxford University Centre for the Environment, using a Dionex Ion Chromatograph, with a sodium carbonate eluant.

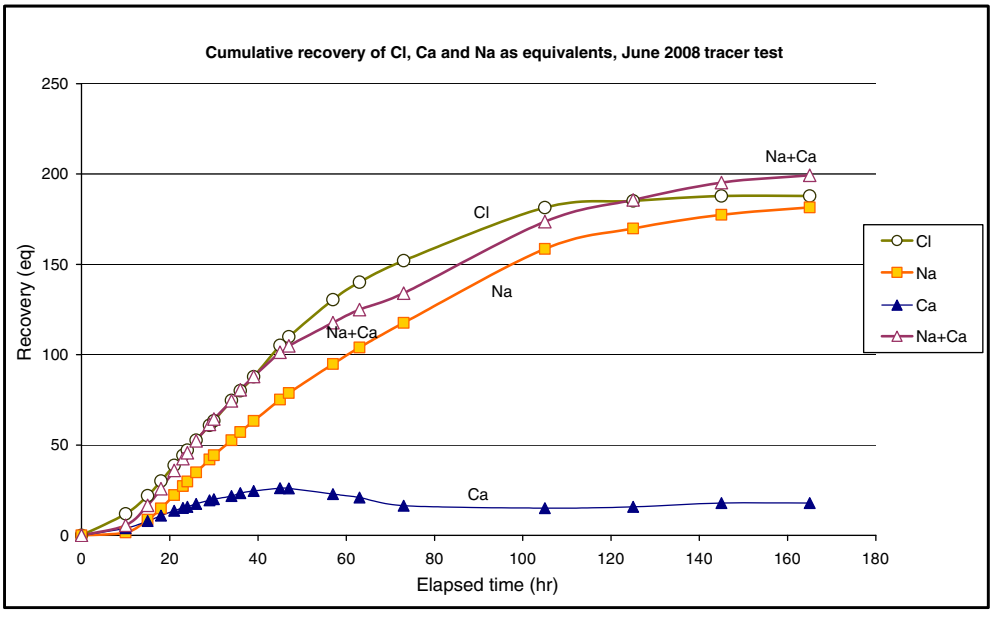

Fig. 7. Cumulative recovery of Cl^-, Na^+ and Ca^{++} (corrected relative to background) in RAPS effluent outfall water during tracer test of June 2008, in equivalents of charge. Calcium was not, of course, applied as a tracer, so the "recovery" is simply calculated as the excess concentration discharged from the RAPS during the course of the test.

- For the elements Ca, Na, Mg, K, Sr, Mn, Fe, Ba by inductively coupled plasma optical emission spectrometry (ICP–OES) at the School of Geography, University of Leeds using a Perkin Elmer Optima 5300 DV.

3. Results and interpretation

3.1. Hydraulic tracer test

In the case of the 25th June 2008 tracer test, monitoring of electrical conductivity shows initial breakthrough of the salt tracer after 6 h, with a peak conductivity after $T_p = 23$ h (Fig. 4). Consideration of T_p implies an apparent modal or dominant tracer velocity of around 1.24×10^{-5} m s^{-1} or 0.0446 m h^{-1}). Conductivity has returned to background after a period of 160–170 h. Applying Eq. (5) with the prevailing flow rate of 0.87 L s^{-1} (specific discharge of 0.0112 m h^{-1}) yields an apparent effective porosity of 25%.

3.2. Hydrochemical observations

Concentrations of major ions were regularly sampled at the outflow of the RAPS (Fig. 5). These were converted to "normalised" concentrations by subtracting the "background" concentrations prior to the commencement of the tracer test (Fig. 6). The mass recovery of chloride within $t = 170$ was calculated at c. 6.7 kg (74%); that of sodium as 4.2 kg (71%), although these figures are dependent on the accuracy of the flow determinations.

Assuming chloride to be the most conservative tracer parameter, Fig. 6 suggests that sodium is very slightly retarded relative to the breakthrough of chloride. More surprisingly, an earlier breakthrough of an excess of calcium (and, to a lesser extent, magnesium) is noted. This calcium excess is followed after an elapsed time of c. 50 h by a relative depletion in calcium. As calcium was not applied as a tracer, these excess and deficit concentrations must relate to calcium being released or absorbed within the RAPS. The Na/Ca meq ratio rises throughout the course of the tracer test. This pattern is strongly suggestive of the pulse of sodium tracer being absorbed onto ion exchange sites (and retarded) in the RAPS matrix and displacing calcium and magnesium (which would be expected to saturate ion exchange sites in a limestone-rich environment). As the salt pulse passes, sodium desorbs from exchange sites and calcium would then be expected to be re-sorbed. Further support for the Ca-Na exchange hypothesis (see also Appelo and Postma, 2005; De Vries, 2007) comes from Fig. 7, where the cumulative recovery of $Na^+ + Ca^{2+}$ (in equivalents) closely matches the Cl^- recovery curve.

4. Modelling the tracer test

Modelling of the tracer test was attempted using three modelling approaches of increasing complexity. The third approach (Section 4.3) is arguably more demanding, in terms of parameterisation, than the available data are able to support. For this reason, even more complex modelling was not felt to be justified.

4.1. Simple advection-dispersion model

A1-dimensional dispersive-advective model (Eq.. (6)) with retardation was selected as a "first pass" algorithm to simulate salt transport downwards through the RAPS. This model was discussed by, e.g., Enfield et al. (1983), and was codified by Banks (1984) and used to simulate the transport of an "initial square-wave" pulse or "slug" of cations through the basal liner of a landfill (conceptually, very similar to the RAPS). The model assumes homogeneity in matrix properties, constant flow velocity and a discrete "slug" of solute of finite length entering the system:

$$C(z,t) = \frac{C_0}{2}\left[erf\left(\frac{z + z_0 - v_s t}{2\sqrt{Dt/R}}\right) - erf\left(\frac{z - v_s t}{2\sqrt{Dt/R}}\right)\right] \quad (6)$$

where

$C(z,t)$ = concentration of solute at depth z and time t
C_0 = initial concentration in slug at $z = 0$ and $t = 0$
z_0 = the initial length of the slug of solute input at the top of RAPS (m)
z = the depth coordinate (m)
v_s = the apparent velocity of the solute (m s^{-1}) = v/R, (or simply v for chloride)
v is the mean linear hydraulic velocity. We have assumed, in the first instance, that the modal velocity H/T_p (1.025 m/23 h = 0.0446 m h^{-1} = 1.24×10^{-5} m s^{-1}) is a reasonable approximation to the mean hydraulic velocity.
erf = the error function
R = retardation factor
D = dispersion coefficient (m^2 s^{-1})
t = time (s) elapsed since tracer injection.

Parameter R: The model was parameterised assuming that R, the retardation factor, for chloride was 1 (i.e. a conservative, non-retarded tracer).

Parameters v and v_s: From the tracer test, if the peak travel time is 23 h and if we assume that this dominant travel time is a first approximation of the mean conservative solute travel time in the mobile pore water fraction, then we can estimate v ($= v_s$ for chloride) as around 1.24×10^{-5} m s^{-1}.

Parameter C_0: The initial concentration of the tracer in the supernatant water lagoon is not known. From Fig. 4, we can see that the initial spike of salt has an electrical conductivity of c. 7200 μS cm^{-1}, relative to background, which corresponds to c. 4000 mg L^{-1} salt at L1 (assuming that c. 550 mg L^{-1} salt is equivalent to 1000 μS cm^{-1}; Hem 1985; Misstear et al. 2006). C_0 can also be estimated using a very simple mixing model. The injected mass of salt was 15×10^6 mg into an estimated RAPS supernatant water volume 280 m^2 × 0.1 m = 28 m^3 = 28.000 L. If mixing were instantaneous, this would result in an average concentration of 536 mg L^{-1} salt (211 mg L^{-1} Na^+ and 325 mg L^{-1} Cl^-).

Parameter z_0:The initial length of the slug z_0 is also highly problematic to parameterise, but one could take two 'extreme' approaches: (i) assume all the salt entered the lagoon, sunk as a dense layer to the base of the lagoon and mixed into a 'bottom layer' of water during the first hour of the test (injection volume = 0.87 L s^{-1} × 3600 s = 3.132 m^3), giving an average thickness of 3.132 m^3/280 m^2 = 1.12 cm, or (ii) assume that the salt mixed throughout the entire c. 0.1 m depth of supernatant water in the lagoon. If the effective porosity of the RAPS is 25%, then we could either postulate (i) a short concentrated slug of length, say, 0.0112 m/0.25 = 0.0447 m (Fig. 8a,b) or (ii) a less concentrated, longer slug of 0.1 m/0.25 = 0.4 m (Fig. 8c,d).

Parameter D: As regards the dispersion coefficient, D, it is not uncommon (Gelhar et al., 1992; Delleur, 1998) to assume a value of c. $0.1 \times L \times v$, where L is the characteristic transport length being considered (in this case $H = 1.025$ m). This approach would yield a starting value of 1.27×10^{-6} m^2 s^{-1} (assuming chemical diffusion is negligible, compared with mechanical dispersion).

Clearly, the application of such a simple 1-D analytical model is optimistic. Nevertheless, Fig. 8 demonstrates that it is possible to obtain a good fit to the early portion of the breakthrough curve with D in the range 1.2 to 2.2×10^{-6} m^2 s^{-1} and an R of 1.15 to 1.2 for sodium. To obtain a fit to the maximum peak height, it is possible either:

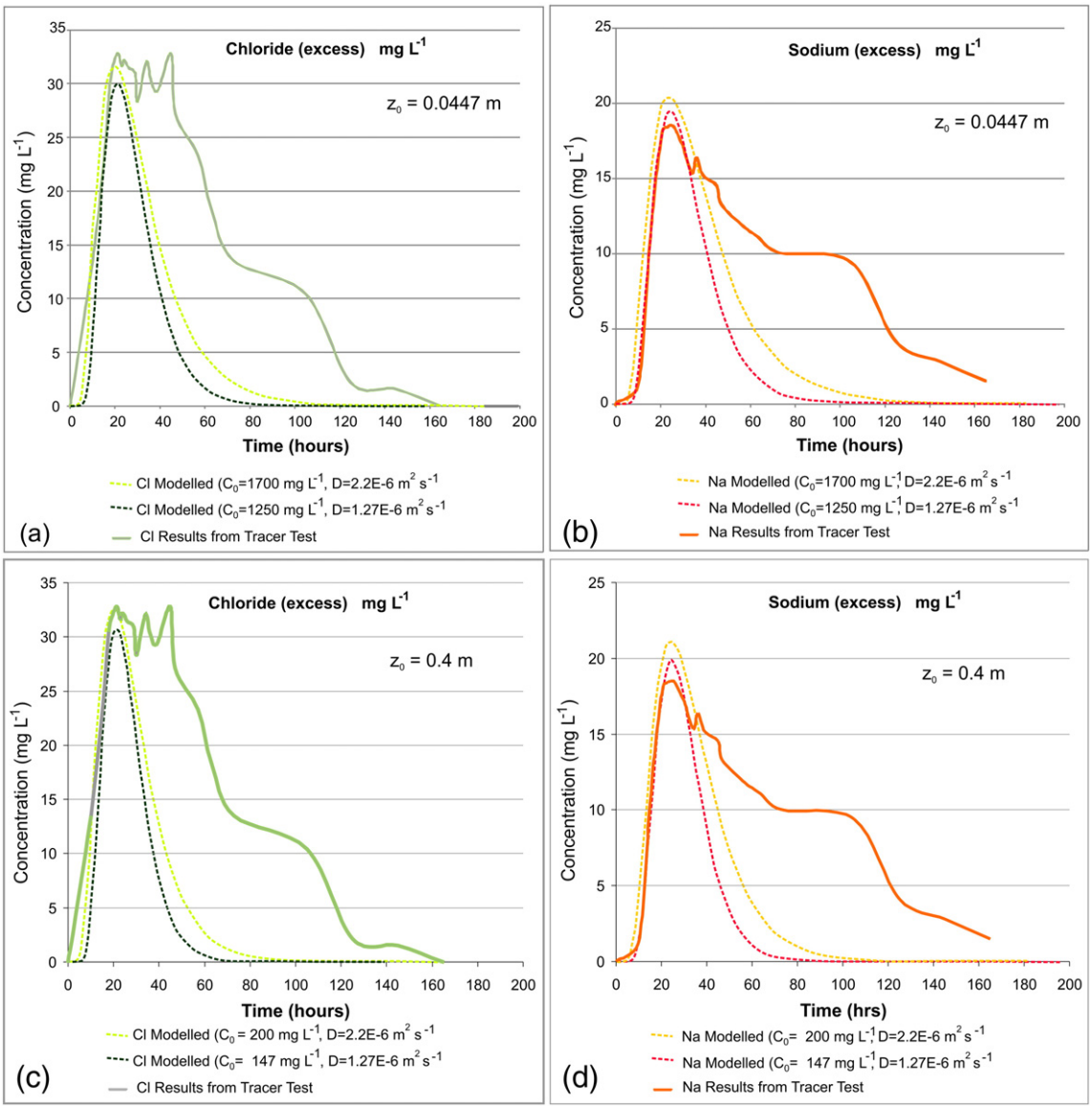

Fig. 8. Modelled versus actual normalised (corrected relative to background) concentrations of (left - a,c) Cl^- and (right - b,d) Na^+ in RAPS effluent water ($z = 1.025$ m) during tracer test of June 2008, using the algorithm of Enfield et al. (1983). Four simulations are shown. Simulation 1 (a) and (b): $C_0 = 1700$ mg L^{-1} NaCl, $R = 1.2$ for sodium and dispersion $= 2.2 \times 10^{-6}$ m^2 s^{-1}; Simulation 2 (a) and (b): $C_0 = 1250$ mg L^{-1} NaCl, $R = 1.15$ for sodium and dispersion $= 1.27 \times 10^{-6}$ m^2 s^{-1}; Simulation 3 (c) and (d): $C_0 = 200$ mg L^{-1} NaCl, $R = 1.2$ for sodium and dispersion $= 2.2 \times 10^{-6}$ m^2 s^{-1}; and Simulation 4 (c) and (d): $C_0 = 147$ mg L^{-1} NaCl, $R = 1.15$ for sodium and dispersion $= 1.27 \times 10^{-6}$ m^2 s^{-1}. For (a) and (b), slug length $z_0 = 0.0447$ m and hydraulic velocity $v = 1.24 \times 10^{-5}$ m s^{-1}, for (c) and (d) $z_0 = 0.4$ m and $v = 1.49 \times 10^{-5}$ m s^{-1}. In all cases $R = 1$ for chloride.

- To set C_0 in the range 1250–1700 mg L^{-1} NaCl (492–669 mg L^{-1} Na^+ and 758–1031 mg L^{-1} Cl^-) with a short slug, or
- To set C_0 in the range 147–200 mg L^{-1} NaCl (58–79 mg L^{-1} Na^+ and 89–121 mg L^{-1} Cl^-) with a long ($z_0 = 0.4$ m) slug. In this latter case, the velocity has to be increased through the RAPS (to 1.49×10^{-5} m s^{-1}) as the long slug takes a longer time to enter the RAPS.

This model produces a poor fit for the latter part of the curve and underestimates the total recovered tracer mass. This poor fit to the late data is unsurprising and is most likely due to three factors:

(i) Too little tracer injected in simulations - the real tracer injection profile to the RAPS is unknown and likely quite complex, potentially with a long, low concentration tail due to mixing (see (ii) below).
(ii) The fact that the model assumes a discrete, well-defined "square wave" slug of tracer uniformly entering the top of the RAPS. In reality, as the tracer initially entered the RAPS, one would have had a localised pulse of high salt concentration entering the RAPS, followed by a more widespread pulse at lower concentration as the salt mixed and diffused throughout the RAPS supernatant water body.
(iii) The likelihood of chemical diffusion of the tracer into micropores within the matrix of the RAPS (i.e. multiple porosity distribution)

Thus, this initial modelling approach might be expected to potentially produce realistic output for the initial tracer breakthrough from the test, but would not be expected to simulate the later (mixing/matrix diffusion-dominated) portion of the test, for which more sophisticated models would be required.

4.2. *Diaz-Goebes and Younger (2004) matrix diffusion model*

Diaz-Goebes and Younger (2004) produced a 1-dimensional model (which is summarised in Eqs. 7–10), which simulates matrix dispersion

Table 2
Parameterisation of the Diaz-Goebes and Younger (2004) matrix diffusion model, with explanations of parameters in Eq.. (7) to (10) and best estimate parameterisations required to yield the curves in Figs. 9 and 10. The selected value of $D_D = 0.0006$ m^2 h^{-1} (1.67×10^{-7} m^2 s^{-1}) is that recommended by Diaz-Goebes and Younger (2004) for other UK salt tracer tests.

Parameter	Fig. 9. instantaneous "spike" model of input	Fig. 10. mixing tank model of input
ψ = partition coefficient between standard advective-dispersive porous medium flow ($\psi = 1$) and matrix diffusion influenced flow ($\psi = 0$)	0.3	0.3
M = mass of tracer injected (kg)	9.75 kg	9.75 kg
n_e = effective porosity of conventional "macro-porous" domain (dimensionless) = v_D/v	25%	19%
n_{mat} = porosity of stagnant micro-porous (matrix) domain (dimensionless)	30%	30%
v_D = specific discharge (Darcy flux) (m s^{-1})	0.00087 m^3 s^{-1}/280 m^2 = 3.11×10^{-6} m s^{-1}	0.00087 m^3 s^{-1}/280 m^2 = 3.11×10^{-6} m s^{-1}
v = linear (hydraulic) water flow velocity (m s^{-1}) = 1.025 m/T_p	0.0446 m h^{-1} = 1.24×10^{-5} m s^{-1}	0.0603 m h^{-1} = 1.67×10^{-5} m s^{-1}
T_p = dominant transit/residence time in RAPS (time to peak concentration)	23 h = 82,800 s	17 h = 61,200 s
D_L = coefficient of longitudinal hydrodynamic dispersion (m^2 s^{-1})	1.27×10^{-6} m^2 s^{-1}	1.27×10^{-6} m^2 s^{-1}
D_e = enhanced dispersion coefficient due to effects of matrix diffusion (m^2 s^{-1})	4.33×10^{-6} m^2 s^{-1}	2.34×10^{-5} m^2 s^{-1}
D_D = coefficient of molecular diffusion within matrix blocks (m^2 s^{-1})	1.67×10^{-7} m^2 s^{-1}	1.67×10^{-7} m^2 s^{-1}
R_{mat} = apparent retardation factor due to matrix diffusion (dimensionless - not chemical sorption)	1.90	2.28
b = characteristic dimension (spacing) of rapid flow domain (m)	0.4 m	0.8 m

effects and allows the user to partition flow between (i) a conventional "macro-porous" medium flow domain and (ii) an equilibrium matrix diffusion domain, via a partition coefficient (which they term ψ). The model was successfully tested by Diaz-Goebes and Younger (2004) on two British RAPS tracer tests and is deemed appropriate for use also at Tan-y-Garn.

$$C(z,t) = \Psi\left[\frac{M}{n_e\sqrt{4\pi D_L t}}\right]\exp\left[\frac{-\left(z-\frac{v_D t}{n_e}\right)^2}{4D_L t}\right] + (1-\Psi) \times \left[\frac{M}{n_e\sqrt{\frac{4\pi D_e t}{R_{mat}}}}\right]\exp\left[\frac{-\left(z-\frac{v_D t}{n_e R_{mat}}\right)^2}{\frac{4D_e t}{R_{mat}}}\right] \quad (7)$$

$$R_{mat} = 1 + \left(\frac{n_{mat}(1-n_e)}{n_e}\right) \quad (8)$$

$$D_e = D_L + \frac{\pi^2 v^2 n_{mat}(1-n_e)}{12 F_t n_e R_{mat}^2} \quad (9)$$

$$F_t = \frac{\pi^2 D_D}{b^2} \quad (10)$$

where parameters are explained in Table 2 and where $C(z,t)$ = concentration of solute (in one dimension - i.e. mass per unit depth) at time t and depth z (kg m^{-1}).

Like Eq. (6), the model assumes homogeneity of the properties of the porous medium within the two domains and a constant flow velocity. Unlike Eq.. (6), the model assumes that the entire tracer (salt) input enters the RAPS instantaneously as a "spike" at time $t = 0$ and depth $z = 0$. Even by applying a 65% recovery correction to the 15 kg salt input and by assuming that 650 mg L^{-1} salt equates to 1000 μS cm^{-1} conductivity, one is only able to broadly approximate the shape of the conductivity signal in the effluent water (Fig. 9).

4.3. *Diaz-Goebes and Younger (2004) model with mixing tank*

The matrix diffusion model (Fig. 9) successfully simulates the general shape of the effluent breakthrough and the "tailing" effect that can be ascribed to matrix diffusion, but still tends to overestimate initial conductivity.

One possible reason for this could be that all tracer is assumed to enter the top of the RAPS at $t = 0$. Thus, the original Diaz-Goebes and Younger (2004) was modified slightly to incorporate a mixing tank effect to the model input. The mixing tank model was based on

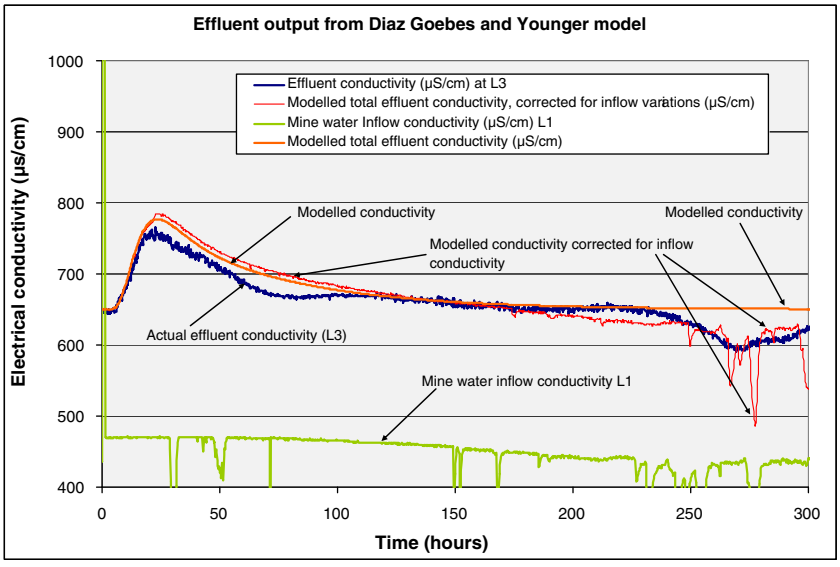

Fig. 9. Output from Diaz-Goebes and Younger (2004) model of Tan-y-Garn tracer experiment, with following input data. Mass of tracer added: 15,000 g × 65% = 9750 g, mean solute transport time in conventional macroporous domain 23 h, RAPS thickness 1.025 m. The "corrected" trace incorporates fluctuations in influent mine water conductivity measured at L1.

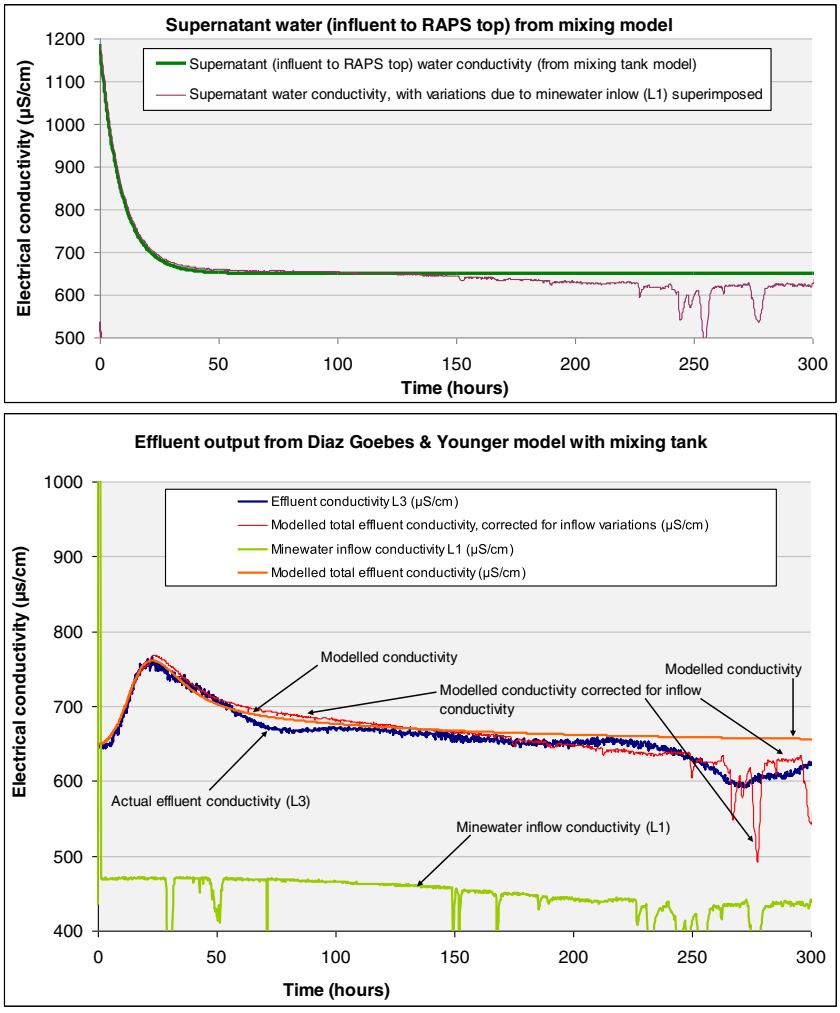

Fig. 10. Output from combined mixing tank/Diaz-Goebes and Younger (2004) model of Tan-y-Garn tracer experiment. (Top) Modelled conductivity of supernatant input water to RAPS by mixing tank model; (bottom) modelled effluent conductivity, with following input data: mass of tracer added: 15,000 g × 65% = 9750 g, mean solute transport time in conventional macroporous domain 17 h, RAPS thickness 1.025 m. The "correction" in both diagrams shows corrections due to fluctuations in influent mine water conductivity measured at L1.

conventional exponential decay of an initial excess tracer concentration C_0 (9750 g/280 m^2/0.1 m = 348 g m^{-3} = 348 mg L^{-1}) by applying a throughflow Q of 0.87 L s^{-1} water and a volume of supernatant lagoon water V_{wat} = 280 m^2 × 0.1 m = 28 m^3.

$$\ln[C(0,t)] = \ln(C_0) - \frac{Qt}{V_{wat}} \quad (11)$$

The new supernatant excess input concentration $C(0,t)$ for a series of 1 h time slices was calculated and the Diaz-Goebes and Younger (2004) model was applied for each time slice. The outputs from each slice were then superimposed to produce a final result.

The number of parameters that are potentially adjustable in this model are considerable and therefore, a unique "best fit" solution could not unambiguously be identified. However, the solution in Fig. 10 provides a very satisfactory fit to the real data. It will be noted that the mean solute travel time for the conventional macroporous domain had to be reduced from 23 to 17 h to obtain a fit. This (as was the case for the long "slug" of tracer in the initial model in Section 4.1) is due to the fact that tracer is entering the RAPS over a prolonged period, leading to the peak effluent tracer concentration apparently being shifted to a later time relative to the start of the tracer application. Thus, failure to account for mixing in the supernatant water initially led to the tracer velocity being underestimated and the travel time being overestimated by around 35% (23 h as opposed to 17 h).

5. Discussion and conclusions

It is important to understand the residence time of water being treated in a RAPS unit in order that the performance can be assessed against design expectations, and that future designs may be improved, e.g. by optimising the design residence time (Kusin et al. 2012; Kusin 2013). RAPS operators need to understand how residence time varies with varying flow rates. Previous tracer tests indicate that the Tan-y-Garn RAPS exhibits a predictable pattern (Fig. 3a), with residence times decreasing proportionately to increasing flows.

During the operational lifetime of the RAPS there is a possibility that hydraulic "short circuits" (preferential flow pathways through the RAPS matrix) could develop or that porosity and hydraulic conductivity could be reduced by compaction or clogging. Changes in hydraulic conductivity can be monitored by simple application of Darcy's Law, by monitoring bulk water throughflow rates and hydraulic head gradients (influent less effluent head) across the RAPS. The existence of short circuits and changes in porosity can be monitored by repeat tracer tests, and by comparing results with the early-life correlation of residence time versus flow rate. Alternatively, such tracer tests could be replaced by monitoring of natural tracer signals such as temperature (Taylor et al., 2016).

The RAPS Tan-y-Garn has performed very satisfactorily at its main task, injecting on average some 2.9 meq L^{-1} alkalinity, and 3.9 meq L^{-1} calcium to the mine water. The RAPS does not behave entirely passively regarding the other components, however: it removes

on average 0.55 meq L^{-1} sulphate from the water, suggesting that sulphate reduction is taking place within the RAPS. Iron has decreased on average by around 1.4 meq L^{-1} through the RAPS, possibly by precipitation as oxyhydroxides at the RAPS top or as sulphides within the RAPS. During the course of its operation, RAPS bulk vertical hydraulic conductivity decreased from around 4 m d^{-1} in 2006 to 0.25 m d^{-1} in 2008.

A sodium chloride tracer test carried out at Tan-y-Garn in June 2008 resulted in peak salt concentrations being detected in RAPS effluent 23 h after salt injection to the raw mine inflow. A retardation of sodium (by a factor of 1.15 to 1.2) relative to chloride was observed, due to reversible cation exchange in the RAPS matrix, resulting in displacement of calcium from ion exchange sites to the effluent water, with concurrent absorption of influent sodium onto exchange sites.

The tracer tests allowed broad estimates of effective porosity (c. 19–32%), hydraulic conductivity (c. 0.25 m d^{-1}), and solute dispersion (1.2 to 2.2 × 10^{-6} m^2 s^{-1}) to be deduced. A simple advection/dispersion model was found adequate to simulate the early portion of the tracer breakthrough curve. A more complex model (Diaz-Goebes and Younger, 2004), which accounted for matrix diffusion processes, was necessary to simulate the long tail of the curve, however. It appears that matrix diffusion processes are of great importance in the RAPS, potentially influencing up to 70% of the solute throughflow. Modelling has further demonstrated that lack of consideration of mixing and dilution processes in the supernatant water can lead to overestimation of real residence times and porosity and underestimation of solute throughflow velocities (in the case of Tan-y-Garn, by a factor of at least some 35%). The real mean throughflow time of the mobile pore water fraction was estimated to be of the order of 17 h (rather than 23 h), due to this effect. Ideally, conductivity or chemical monitoring of the supernatant water during the course of the test would have assisted in defining the tracer input signal.

Acknowledgement

This research was carried out as part of a dissertation whilst the main author was studying at the University of Leeds, UK. The support of academic staff at the School of Earth and Environment is gratefully acknowledged. Meteorological data used in Fig. 4b supplied by the UK Met Office under terms of licence 010070604.

References

Aldous, P.J., Smart, P.L., 1988. Tracing ground-water movement in abandoned coal mined aquifers using fluorescent dye. Ground Water 26, 172–178. http://dx.doi.org/10.1111/j.1745-6584.1988.tb00380.x.

Amos, P., Younger, P.L., 2003. Substrate characterisation for a subsurface reactive barrier to treat colliery spoil leachate. Water Res. 37, 108–120. http://dx.doi.org/10.1016/S0043-1354(02)00159-8.

Appelo, C.A.J., Postma, D., 2005. Geochemistry, Groundwater and Pollution. second ed. A.A. Balkema, Leiden.

Atkins, 2006. The Coal Authority: Tan-y-Garn Mine Water Treatment Scheme Operation and Maintenance Manual. Atkins Ltd., Report 5001064/69-OM for the Coal Authority, July 2006. Atkins Global, Birmingham, UK.

Atkins, 2007. Tan y Garn South Wales: Review of the Performance of the Tan y Garn Mine Water Treatment System: Summary Report. Atkins Ltd., Report 5046550/Tan y Garn RAPS, for the Coal Authority, August 2007. Atkins Global, Birmingham, UK.

Banks, D., 1984. An investigation into the suitability of glacial sands, clays and gravels for use as basal liners of a landfill site MSc dissertation. Dept. of Geological Sciences, University of Birmingham, UK.

Banks, S.B., Banks, D., 2001. Abandoned mines drainage: impact assessment and mitigation of discharges from coal mines in the UK. Eng. Geol. 60, 31–37. http://dx.doi.org/10.1016/S0013-7952(00)00086-7.

Bernier, L., Aubertin, M., Dagenais, A.M., Bussière, B., Bienvenu, L., Cyr, J., 2001. Limestone drain design criteria in AMD passive treatment: theory, practice and hydrogeochemistry monitoring at Lorraine mine site, Temiscamingue. Proc. Annual Meeting of the Canadian Institute of Mining Metallurgy and Petroleum (CIM), "Minespace 2001" Technical paper 48, 9 pp. CIM, April 29th–May 2nd 2001, Quebec, Canada.

BGS, 1977. Sheet 230 Ammanford (Solid). Geological Survey of Great Britain (England and Wales). British Geological Survey. Geological map1:50,000 series.

Coal Authority, 2014. Tan-y-Garn mine water treatment scheme. http://coal.decc.gov.uk/en/coal/cms/environment/schemes/tan_y_garn/tan_y_garn.aspx (Accessed 2 May 2014).

Cravotta, C.A., Trahan, M.K., 1999. Limestone drains to increase pH and remove dissolved metals from acidic mine drainage. Appl. Geochem. 14, 581–606. http://dx.doi.org/10.1016/S0883-2927(98)00066-3.

Davies, D., 1921. The ecology of the Westphalian and the lower part of the Staffordian series of the Clydach Vale and Gilfach Goch (East Glamorgan). Q. J. Geol. Soc. Lond. 77, 30–74. http://dx.doi.org/10.1144/GSL.JGS.1921.77.01-04.05.

de Vries, J.J., 2007. Groundwater. In: Wong, T.E., Batjes, D.A.J., de Jager, J. (Eds.), "Geology of the Netherlands". Royal Netherlands Academy of Arts and Sciences, pp. 295–315.

Delleur, J.W., 1998. Elementary groundwater flow and transport processes. In: Delleur, J.W. (Ed.), The Handbook of Groundwater Engineering. CRC Press Boca Raton, USA.

Diaz-Goebes, M., Younger, P.L., 2004. A simple analytical model for interpretation of tracer tests in two-domain subsurface flow systems. Mine Water Environ. 23, 138–143. http://dx.doi.org/10.1007/s10230-004-0054-y.

Doyen, P.M., 1988. Permeability, conductivity, and pore geometry of sandstone. J. Geophys. Res. Solid Earth 93 (B7), 7729–7740. http://dx.doi.org/10.1029/JB093iB07p07729 (1978–2012).

Enfield, C.G., Carsel, R.F., Cohen, S.Z., Phan, T., Walters, D.M., 1983. Approximating pollutant transport to ground water. Ground Water 6, 711–720. http://dx.doi.org/10.1111/j.1745-6584.1982.tb01391.x.

Fabian, D., Aplin, A.C., Younger, P.L., 2005. Geochemical performance of a reducing and alkalinity-producing system (RAPS) for the passive treatment of acidic mine drainage at Bowden close, United Kingdom. In: Loredo, J., Pendás, F. (Eds.), Mine Water 2005 – Mine Closure, Proc. 9th International Mine Water Association Congress (IMWA), Oviedo, Spain, pp. 383–387.

Gelhar, L.W., Welty, C., Rehfeldt, K.R., 1992. A critical review of field-scale dispersion in aquifers. Water Resour. Res. 28, 1955–1974. http://dx.doi.org/10.1029/92WR00607.

Geroni, J.N., 2011. Rates and Mechanisms of Chemical Processes Affecting the Treatment of Ferruginous Mine Water PhD School of Engineering, Cardiff University, UK, http://orca.cf.ac.uk/19120/1/2011GeroniJNPhD.pdf (Accessed 2 May 2014).

Geroni, J.N., Sapsford, D.J., Florence, K., 2011. Degassing CO_2 from mine water: implications for treatment of circumneutral drainage. In: Rüde, T.R., Freund, A., Wolkersdorfer, C. (Eds.), Mine Water - Managing the Challenges, Proc. 11th International Mine Water Association Congress (IMWA) 2011, Aachen, Germany, pp. 319–324.

Greenwell, A., Elsden, J.V., 1907. Analyses of British Coals and Coke. Chichester Press, London 456 pp.

Harrison, D.J., 1993. High-purity limestones in England and Wales. Q. J. Eng. Geol. Hydrogeol. 26, 293–303. http://dx.doi.org/10.1144/GSL.QJEGH.1993.026.004.05.

Hedin, R.S., Nairn, R.W., Kleinmann, R.L.P., 1994a. Passive treatment of polluted coal mine drainage. Bureau of Mines Information Circular 9389. United States Department of Interior, Washington DC.

Hedin, R.S., Watzlaf, G.R., Nairn, R.W., 1994b. Passive treatment of acid mine drainage with limestone. J. Environ. Qual. 23, 1338–1345. http://dx.doi.org/10.2134/jeq1994.00472425002300060030x.

Heiderscheidt, J.L., Crimi, M., Siegrist, R.L., Singletary, M.A., 2008. Optimization of full-scale permanganate ISCO system operation: laboratory and numerical studies. Ground Water Monit. Rem. 28 (4), 72–84. http://dx.doi.org/10.1111/j.1745-6592.2008.00213.x.

Hem, J.D., 1985. Study and Interpretation of the Chemical Characteristics of Natural Water. US Geological Survey Water-Supply Paper 2254, Washington DC, third ed.

Kepler, D.A., McCleary, E.C., 1994. Successive alkalinity producing systems (SAPS) for the treatment of acidic mine drainage. Proceedings of the International Land Reclamation and Mine Drainage Conference and the 3rd International Conference on the Abatement of Acidic Drainage. 1, pp. 195–204 (Pittsburgh, April 1994).

Kusin, F.M., 2013. A review of the importance of hydraulic residence time on improved design of mine water treatment systems. World Appl. Sci. J. 26 (10), 1316–1322. http://dx.doi.org/10.5829/idosi.wasj.2013.26.10.412.

Kusin, F.M., Jarvis, A.P., Gandy, C.J., 2012. Hydraulic performance assessment of passive coal mine water treatment systems in the UK. Ecol. Eng. 49, 233–243. http://dx.doi.org/10.1016/j.ecoleng.2012.08.008.

Lee, C., 1995. When coal came from the Rhondda. Teach. Earth Sci. 20, 123–128.

McAllan, J., Banks, D., Beyer, N., Watson, I., 2009. Alkalinity, temporary (CO_2) and permanent acidity: an empirical assessment of the significance of field and laboratory determinations on mine waters. Geochem. Explor. Environ. Anal. 9, 299–312. http://dx.doi.org/10.1144/1467-7873/09-193.

Misstear, B., Banks, D., Clark, L., 2006. Water Wells and Boreholes. Wiley, Chichester (514 pp. ISBN/ISSN: 978-0-470-84989).

PIRAMID Consortium, 2003. Engineering guidelines for the passive remediation of acidic and/or metalliferous mine drainage and similar wastewaters. European Commission 5th Framework RTD Project no. EVK1-CT-1999-000021 "Passive *in-situ* Remediation of Acidic Mine/Industrial Drainage" (PIRAMID). University of Newcastle Upon Tyne, Newcastle Upon Tyne, UK, http://www.imwa.info/piramid/files/PIRAMIDGuidelinesv10.pdf (Accessed 14 January 2014).

Rezaee, M.R., Jafari, A., Kazemzadeh, E., 2006. Relationships between permeability, porosity and pore throat size in carbonate rocks using regression analysis and neural networks. J. Geophys. Eng. 3, 370–376. http://dx.doi.org/10.1088/1742-2132/3/4/008.

Sapsford, D.J., Watson, I., 2011. A process-orientated design and performance assessment methodology for passive mine water treatment systems. Ecol. Eng. 37, 970–975. http://dx.doi.org/10.1016/j.ecoleng.2010.12.010.

Spears, D.A., Rippon, J.H., Cavender, P.F., 1999. Geological controls on the sulphur distribution in British Carboniferous coals: a review and reappraisal. Int. J. Coal Geol. 40, 59–81. http://dx.doi.org/10.1016/S0166-5162(98)00057-3.

SRK, 1994. Study of ferruginous mine water impacts in Wales. Phase 2a Determination of remedial options; volume 2 - site reports. Steffen, Robertson and Kirsten (UK) Ltd, Cardiff, Wales Report ADM/489 AC001.REP. September 1994.

Strahan, A., Cantrill, T.C., Thomas, H.H., 1907. The geology of the South Wales coal-field Part VII: The Country around Ammanford. Memoirs of the Geological Survey, England and Wales. HMSO, London.

Taylor, K., 2008. A Combined Thermal and Chemical Tracer Test to Assess Residence Times in a Passive Mine Water Treatment System, South Wales MSc dissertation. School of Earth and Environment, University of Leeds, UK.

Taylor, K., Banks, D., Watson, I., 2016. Heat as a natural, low-cost tracer in mine water systems: The attenuation and retardation of thermal signals in a reducing and alkalinity producing treatment system (RAPS). Int. J. Coal Geol. 164, 47–56.

Wandless, A.M., 1959. The occurrence of sulphur in British coals. J. Inst. Fuel 32, 258–266.

Watson, I.A., Taylor, K., Sapsford, D.J., Banks, D., 2009. Tracer testing to investigate hydraulic performance of a RAPS treating mine water in South Wales. Proceedings of the 8th International Conference on Acid Rock Drainage - ICARD (Securing the Future), 23rd-26th June 2009, Skellefteå, Sweden, pp. 762–771.

Watzlaf, G.R., Schroeder, K.T., Kairies, C.L., 2000a. Long-term performance of anoxic limestone drains. Mine Water Environ. 19, 98–110. http://dx.doi.org/10.1007/BF02687258.

Watzlaf, G.R., Schroeder, K.T., Kairies, C., 2000b. Long-term performance of alkalinity producing passive systems for the treatment of mine drainage. Proceedings of the 2000 National Meeting of the American Society for Surface Mining and Reclamation, Tampa, Florida, 11th–15th June 2000, 262–274 http://www.asmr.us/Publications/Conference%20Proceedings/2000/Watzlaf%20262-274.pdf (Accessed 14 January 2014).

Wolkersdorfer, C., 2002. Mine water tracing. Geol. Soc. Lond. Spec. Pub. 198, 47–61. http://dx.doi.org/10.1144/GSL.SP.2002.198.01.03.

Wolkersdorfer, C., 2008. Water Management at Abandoned Flooded Underground Mines - Fundamentals, Tracer Tests, Modelling, Water Treatment. Springer, Heidelberg http://dx.doi.org/10.1007/978-3-540-77331-3.

Wolkersdorfer, C., Hasche, A., Göbel, J., Younger, P.L., 2005. Tracer test in the Bowden Close passive treatment system (UK) - preliminary results. Wiss. Mitt. 28, 87–92 (Institut für Geologie, Freiberg) http://www.wolkersdorfer.info/publication/pdf/BowdenClose.pdf (Accessed 14 January 2014).

Wolkersdorfer, C., Göbel, J., Hasche-Berger, A., 2016. Assessing subsurface flow hydraulics of a coal mine water bioremediation system using a multi-tracer approach. Int. J. Coal Geol. 164, 57–67.

Younger, P.L., Banwart, S.A., Hedin, R.S., 2002. Mine Water: Hydrology, Pollution, Remediation. Kluwer Academic Publishers, Dordrecht.